



Kinetic study of ethane oxydehydrogenation over AIPO-5

Juinn Yao Wu, and Ben Zu Wan

Ind. Eng. Chem. Res., 1993, 32 (12), 2987-2990 • DOI: 10.1021/ie00024a005

Downloaded from http://pubs.acs.org on November 26, 2008

More About This Article

The permalink http://dx.doi.org/10.1021/ie00024a005 provides access to:

- Links to articles and content related to this article
- Copyright permission to reproduce figures and/or text from this article



Kinetic Study of Ethane Oxydehydrogenation over AlPO-5

Juinn-Yao Wu and Ben-Zu Wan*

Department of Chemical Engineering, National Taiwan University, Taipei, Taiwan, Republic of China

The kinetics of ethane oxydehydrogenation to produce ethylene over AlPO-5, a member of the aluminophosphate molecular sieve family, has been investigated over the temperature range 748–798 K at atmospheric pressure. It was observed that parallel reactions to ethylene and carbon oxides occur on the surface. A kinetic model involving oxygen adsorption was proposed for the ethane oxydehydrogenation. On the basis of the kinetic analysis, it is suggested that the reactions of ethane on the surface through two different sites are the rate-determining step. The apparent activation energy was 83 kcal mol⁻¹. For oxygen adsorption on the surface, the changes of enthalpy and entropy were -23 kcal mol⁻¹ and -25 cal mol⁻¹ K⁻¹, respectively. These explain the adsorption phenomena reasonably.

Introduction

Microporous aluminophosphate, with diverse structural features, has been synthesized successfully (Wilson et al., 1982). AlPO-5 is a member of the aluminophosphate molecular sieve family. Its straight cylindrical channels with 0.7-nm pore opening are composed of 12-member rings of regular alternation of Al and P in the tetrahedral framework of AlPO-5 (Bennett et al., 1986). The advantages of AlPO-5 in the catalytic reaction are heat stability and straight channels with large openings, preventing coke deposition. The weak point in AlPO-5 as a catalyst is that AlPO-5 is an electrically neutral structure without ionexchanging capability and with low acidity. It was reported that partial substitution of other elements with different valences (such as silicon, gallium, and some transition metals) for aluminum or phosphorus could give rise to Brønsted acidic sites in the framework (Lok et al., 1984; Wilson and Lanigen, 1986).

In ethane oxydehydrogenation into ethylene, it was found that AlPO-5 and MAPO-5—some of the first-row transition metals (e.g., Mn, Fe, Ni, V, and Cu) are substituted into the framework of AlPO-5—were selectively active (Wan et al., 1991; Wan and Huang, 1991). It was impressive that the selectivity of ethylene was higher than 80% in ethane oxydehydrogenation over AlPO-5 at 723 and 773 K. Even though the electrically neutral structure of AlPO-5 was not expected to exhibit any acidity, the surface hydroxyl group (Al–OH and P–OH) may possess some residual hydrophilic and catalytic character due to the local electronegativity differences between Al³+ and P⁵+ (Hedge et al., 1987).

In this work, the reaction model of ethane oxydehydrogenation into ethylene over AlPO-5 was determined through kinetic study, in order to understand how ethane oxydehydrogenated over AlPO-5 to produce ethylene selectively. From this proposed model, the changes of enthalpy and entropy for the oxygen adsorption on the surface were examined.

Experimental Section

AlPO-5 was prepared following the hydrothermal crystallization method (Wan et al.,1991). The resultant catalyst was characterized by XRD (Phillips PW1729 with CuK α radiation) and BET surface area (Micromeritic Accusorb 2100D unit).

Ethane oxydehydrogenation was carried out in a fixed bed differential type reactor (12-mm-o.d. quartz tube). The flow rates of ethane, air, and nitrogen were controlled and read by mass controllers and meters (Brooks 5850 and 5878). The maximum controlled flow rates of ethane and nitrogen were 25 mL/min, and that of air was 48 mL/min. The reaction temperatures were controlled in the range 748-798 K by a PID temperature controller. Before each reaction, the catalyst was pretreated at 823 K for more than 2 h under air flow. An on-line China Chromatography 8700T chromatograph with Porapak S column was used to separate carbon dioxide and ethylene from the product stream. Another Shimadzu GC-8A gas chromatograph with a 5A Molecular Sieve column was used to separate carbon monoxide.

In the observation of product distributions at different contact times, ethane and air at ratio of 1/2 at 1 atm of total pressure were fed into the quartz tube reactor containing 0.6 g of catalyst. The total flow rates were changed under the range 18-72~mL/min. In the reaction kinetic measurements, 0.6 g of catalyst and a 50 mL/min total flow rate were used. The partial pressure of ethane was changed within 0.1-0.5 atm, and that of oxygen (from air) was changed within 0.02-0.1 atm. The carbon selectivity was calculated on a carbon basis and was defined as selectivity of a given product = (moles of the given product × number of carbon atoms in the molecular formula)/(moles of ethane consumed \times 2). Due to the fact that the conversion of each reactant was maintained at less than about 15%, the consumption rate of ethane (-r) was defined as the reaction rate in a differential reactor, -r = FX/W (Froment and Bischoff, 1979), where F is the input mole flow rate of ethane, X is the ethane conversion, and W is the catalyst weight. The production rate of a specific product was the consumption rate of ethane times the selectivity of this product.

Results

Water and three carbon products (ethylene, carbon monoxide, and carbon dioxide) were found in the reactions. Under the reaction temperature of 773 K, the carbon selectivities of products maintained constant levels at ethane conversions of 1.0–6.5% (Figure 1). Ethylene selectivity was about 80%, carbon monoxide selectivity was about 15%, and carbon dioxide selectivity was about 5%. The result indicates that ethane oxydehydrogenation to ethylene and oxidation to carbon monoxide and carbon dioxide were parallel reactions over AlPO-5. Thus, the

^{*} To whom correspondence should be addressed.

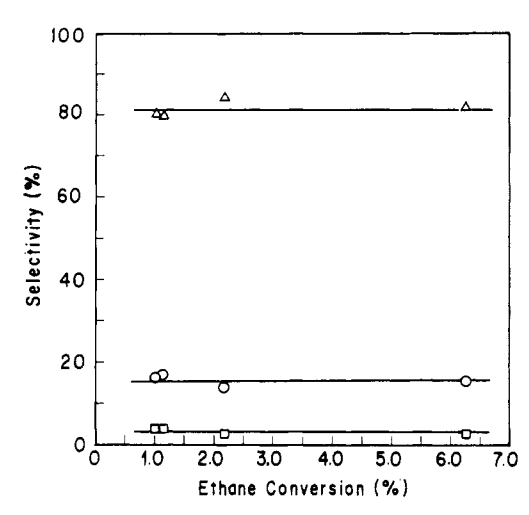


Figure 1. Product selectivity vs ethane conversion over AlPO-5 at 775 K and 50 mL/min total flow rate (air/ethane = 2): $O, CO; \Box, CO_2;$ Δ , C_2H_4 .

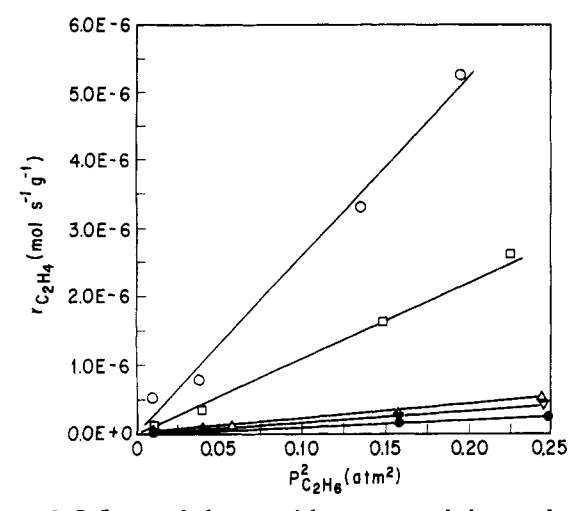


Figure 2. Influence of ethane partial pressure on ethylene production rate over AlPO-5. Total flow rate = 50 mL/min; oxygen pressure = 0.1 atm: O, 798 K; □, 783 K; △, 773 K; ⋄, 758 K; ●, 748 K.

following kinetic analysis of ethane oxydehydrogenation was made by the measurement of ethylene production rate. The influence of ethane partial pressure on oxydehydrogenation rate over AlPO-5 at different reaction temperatures is shown in Figure 2. The linear relationship between reaction rate and square of ethane partial pressure implies that ethane oxydehydrogenation over AlPO-5 is a second-order reaction to ethane partial pressure. Figure 3 shows the influence of oxygen partial pressure on oxydehydrogenation rate over AlPO-5 under the same temperature range. It seems that when the oxygen partial pressure was larger than 0.02 atm it did not affect the ethane oxydehydrogenation rate at lower reaction temperatures (748, 758, and 773 K). At higher reaction temperatures (783 and 798 K), the oxydehydrogenation rates were increased with increasing oxygen partial pressures and then approached a steady level at higher oxygen partial pressures. In fact, sufficient oxygen is indeed necessary in the reaction. When no oxygen was added, no reaction occurred under the reaction conditions studied in this research.

Kinetic Model Development

The data of reaction rates in relation to reactant partial pressures are listed in Table I. The kinetic models were

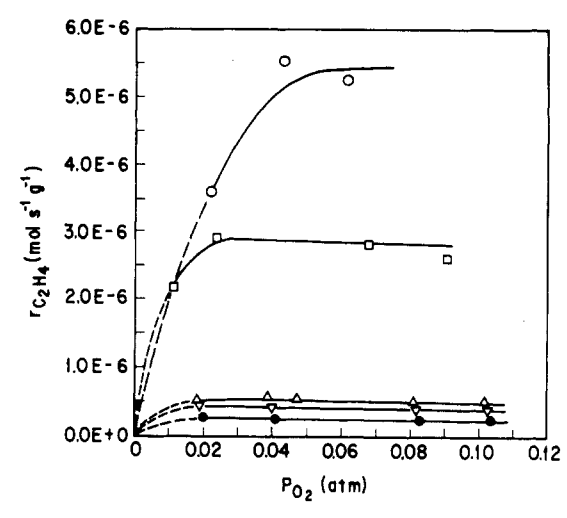


Figure 3. Influence of oxygen partial pressure on ethylene production rate over AlPO-5. Total flow rate = 50 mL/min; ethane pressure = 0.5 atm: O, 798 K; □, 783 K; △, 773 K; ⋄, 758 K; ●, 748 K.

Table I. Experimental Data of Ethylene Production Rate

at Different Reactant Partial Pressures			
T/K	$r_{\mathrm{C_2H}}/\mathrm{mol}\;\mathrm{s}^{-1}\;\mathrm{g}^{-1}$	po ₂ /atm	$p_{\mathrm{C_2H_0}}/\mathrm{atm}$
748	$2.54\mathrm{E}{-7^a}$	0.104	0.498
	1.5 4E -7	0.104	0.397
	4.76E-8	0.105	0.199
	1.55E-8	0.105	0.100
	2.48E-7	0.083	0.498
	2.45E-7	0.041	0.498
	2.68E-7	0.020	0.498
758	4.02 E -7	0.103	0.496
	2.60E-7	0.103	0.397
	6.32E-8	0.104	0.199
	1.56E-8	0.105	0.100
	3. 94E- 7	0.082	0.496
	3.97E-7	0.040	0.496
	4.43E-7	0.019	0.496
773	5.41 E -7	0.102	0.494
	3.17E-7	0.103	0.398
	1.18E-7	0.104	0.239
	1.52E-8	0.105	0.100
	5.37E-7	0.081	0.495
	5.62E-7	0.048	0.494
	5.72E-7	0.039	0.494
	5.22E-7	0.018	0.495
	3.24E-7	0.040	0.397
	1.04E-7	0.041	0.239
	7.73E-8	0.041	0.199
	1.60E-8	0.042	0.100
	7.39 E -8	0.167	0.199
	8.40E-8	0.125	0.199
	8.15 E -8	0.083	0.199
	7.26E-8	0.062	0.199
783	2.61E-6	0.091	0.475
	1.62E-6	0.097	0.385
	3.34E-7	0.103	0.197
	1.08E-7	0.104	0.099
	2.81E-6	0.068	0.473
	2.89E-6	0.024	0.471
	2.15E-6	0.011	0.479
798	5.24E-6	0.062	0.442
	3.29E-6	0.085	0.367
	7.72 E -7	0.101	0.193
	5.09 E -7	0.104	0.095
	5.52E-6	0.043	0.441
	3.59E-6	0.022	0.464

^a Read as 2.54×10^{-7} .

developed to fit these data statistically. Several mechanisms, including Langmuir-Hinshelwood types with molecular or atomic adsorption on a single site or dual sites, an Eley-Rideal type for adsorption, and a reductionoxidation type, have been examined. The approach steps

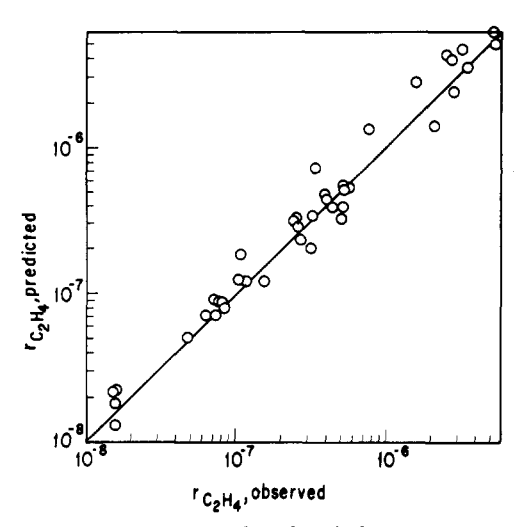


Figure 4. Comparison of predicted and observed values of C₂H₄ production rates over AlPO-5.

used to justify a proposed model were as follows: At first, basic rate equations were obtained by assuming that each step in the proposed mechanism was the rate-determining step. Second, simplification of each rate equation was made by some rational assumptions. Finally, linear regressions of the consequent equations were made at each temperature to obtain the rate constants and adsorption constants. When any of the derived constants from regression was negative, that rate equation was eliminated.

It was found that the only model which could fit the kinetic data well was

$$O_2 + s \rightleftharpoons O_2 s$$
 (1)

$$C_0H_6 + s \rightleftharpoons C_0H_6s$$
 (2)

$$C_2H_6 + O_2s \rightleftharpoons C_2H_6O_2s \tag{3}$$

$$C_9H_8S + C_9H_8O_9S \rightleftharpoons 2C_9H_4 + 2H_9O + 2s$$
 (4)

where s represents an active site on the catalyst. By assuming that the fourth step was the rate-determining step and the adsorption equilibrium constants of ethane were much smaller than those of oxygen, the rate equation was formulated as follows:

rate =
$$\frac{k_4 C_t^2 K_1 K_2 K_3 P_{O_2} P_{C_2 H_6}^2}{(1 + K_1 P_{O_c})^2}$$
(5)

where P represents the partial pressure, C_t is the total number of active sites on the catalyst surface for ethane oxydehydrogenation, K_1 is the equilibrium constant of oxygen adsorption on the active sites of catalyst, K_2 and K_3 are both equilibrium constants of ethane adsorption on the sites either without or with oxygen, and k_4 is the rate constant of surface reaction between two intermediates in the fourth reaction step. Figure 4 shows how agreeable the rate data from experiment are with those estimated from this rate equation. The mean deviation error was about 24.9%. The random distribution around the diagonal equivalent line of empirical and calculated values of rate suggests that this rate equation describes the experimental result quite well.

Discussion

The values of $k_4C_t^2K_2K_3$ and K_1 at different reaction temperatures obtained from the linear regression are listed

Table II. Rate Constants and Oxygen Adsorption **Equilibrium Constants at Different Reaction Temperatures**

T/K	$k_4 C_{ m t}^2 K_2 K_3 / { m mol~g^{-1}~s^{-1}~atm^{-2}}$	$K_{1}/\mathrm{atm^{-1}}$
748	5.34E-6a	14.82
758	8.11E-6	19.19
773	9.16E-6	16.09
783	7.55 E -5	8.75
798	1.51E-4	6.38

^a Read as 5.34×10^{-6} .

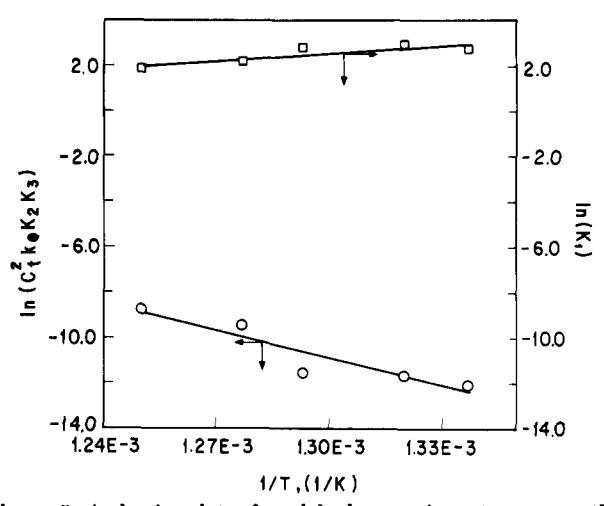


Figure 5. Arrhenius plots of oxydehydrogenation rate constant (E_a = 83 kcal mol⁻¹, γ = 0.93) and oxygen absorption equilibrium constant $(\Delta H = -23 \text{ kcal mol}^{-1}, \Delta S = -25 \text{ cal mol}^{-1} \text{ K}^{-1}, \gamma = 0.85) \text{ over AlPO-5}.$

in Table II. These two reaction parameters can be expressed as a function of temperature:

$$k_{A}C_{+}^{2}K_{2}K_{3} = A \exp(-E_{p}/RT)$$
 (6)

$$K_1 = \exp(\Delta S/R) \exp(-\Delta H/RT) \tag{7}$$

Here, E_a is the apparent activation energy, A is the Arrhenius constant, and ΔH and ΔS are the enthalpy change and the entropy change for molecular oxygen adsorption, respectively. From Figure 5, the parameters in eqs 6 and 7 were estimated as $E_a = 83$ kcal mol⁻¹, ΔH = -23 kcal mol⁻¹, and ΔS = -25 cal mol⁻¹ K⁻¹. The linear correlation factors, γ , of the two lines in Figure 5 are 0.93 and 0.85, respectively, which suggests an acceptable linear relationship in the plots ($\gamma = 1$ represents a perfect linear relationship).

The predicted value of E_a is somewhat higher than that one of a general catalytic reaction. It elucidates that the reaction is sensitive to the reaction temperature. That is, when the reaction temperature is higher, the ethane oxydehydrogenation rate is more rapid. On the other hand, the reaction seemed to be close to a homogeneous reaction because the apparent activation energy was close to the bonding energy of either a carbon-carbon or a carbonhydrogen bond. However, the conversion of 0.13% of a blank test (under conditions that the total flow rate was 36 mL/min, the air/ethane mole ratio was 2, and the reaction temperature was 773 K) was much smaller than the conversion of 2.46% of a catalytic reaction under the same conditions with 0.6 g of AlPO-5. It is obvious that the reaction on the surface of catalyst was the dominating reaction and that the reaction needs the AlPO-5 surface to accelerate the reaction rate. Furthermore, the negative values of ΔH and ΔS indicate that the adsorption of oxygen is an exothermic reaction, and the entropy of the system decreases after oxygen adsorption on the catalyst surface. This is consistent with the general adsorption phenomena.

AlPO-5 has a channel structure similar to that of HZSM-5, which consists of a tetrahedral silica-alumina network and Brønsted acidic sites from bridged hydroxyl groups on the surface. In a study of surface defects on HZSM-5 by Shih (1983), it was found that, during the reaction of HZSM-5 and oxygen at high temperature, the zeolite surface produces positive holes on oxygen atoms, called solid-state defects. It was demonstrated that these positive holes would interact with the ionizable organic molecule adsorbed on the zeolite surface to produce the active radical cation. On the other hand, it has been verified that there were terminal hydroxyl groups on the external surface of AlPO-5 with the structure of alternating aluminum and phosphorus tetrahedra (Hedge et al., 1987). It also exhibited weak Brønsted acidic sites. In our results, we found that oxygen played an important role in the reaction of ethane oxydehydrogenation over AlPO-5. It may be just like HZSM-5 and produce positive holes on the AlPO-5 surface when interacting with oxygen. Then the positive holes reacted with ethane and formed ethyl radical cation on the catalyst surface, followed by the dehydrogenation of the radical with oxygen to produce ethylene.

Conclusion

From this study, it is concluded that ethane oxydehydrogenation can occur on the surface of AlPO-5, although it is generally recognized that the surface is rather neutral and inert.

Under the reaction conditions used in this study, the rate of ethane oxydehydrogenation over AlPO-5 was expressed as

rate =
$$\frac{k_4 C_t^2 K_1 K_2 K_3 P_{O_2} P_{C_2 H_6}^2}{(1 + K_1 P_{O_2})^2}$$

From the proposed reaction model, it seems that oxygen can be adsorbed on AIPO-5. The reactions of ethane on

the surface are through two different sites: one originates from the AlPO-5 surface and the other from the AlPO-5 surface with adsorbed oxygen.

Acknowledgment

Financial support from the National Science Council in Taiwan, R.O.C., under contract No. NSC81-0402-E002-20 is greatly appreciated.

Literature Cited

Bennett, J. M.; Dytrych, W. J.; Pluth, J. J.; Richardson, J. W.; Smith, J. V. Structural Features of Aluminophosphate Materials with Al/P=1. Zeolites 1986, 6, (Sept), 349-361.

Froment, G. F.; Bischoff, K. B. Kinetics of Heterogeneous Catalytic Reaction. In Chemical Reactor Analysis and Design, 2nd ed.; John Wiley & Sons: New York, 1979; Chapter 2, p 86.

Hedge, S. G.; Ratnasamy, P.; Kustov, L. M.; Kazansky, V. B. Acidity and Catalytic Activity of SAPO-5 and AlPO-5 Molecular Sieves. Zeolites 1988, 8, (March), 137-141.

Lok, B. M.; Messina, C. A.; Patton, R. L.; Gajek, R. T.; Cannan, T. R.; Flanigen, E. M. Crystalline Metal Aluminophosphates. U.S. Patent 4,440,871, 1984.

Shih, S. Chemical Reactions of Alkenes and Alkynes with Solid-State Defects on ZSM-5. J. Catal. 1983, 79, 390-395.

Wan B.; Huang, K. MnAPO-5 as A Catalyst for Ethane Oxydehydrogenation. Appl. Catal. 1991, 73, 113-124.

Wan, B.; Huang, K.; Yang, T. C.; Tai, C. Characterization and Catalytic Properties of MAPO-5. J. Chin. Inst. Chem. Eng. 1991, 22(1), 17-23.

Wilson, S. T.; Lok, B. M.; Messina, C. A.; Cannan, T. R.; Flanigen, E. M. Aluminophosphate Molecular Sieves: A New Class of Microporous Crystalline Inorganic Solids. J. Am. Chem. Soc. 1982, 104, 1146-1147.

Wilson, S. T.; Flanigen, E. M. Crystalline Silicoaluminophosphosphates. U.S. Patent 4,567,029, 1986.

Received for review March 4, 1993 Revised manuscript received August 6, 1993 Accepted August 19, 1993

Abstract published in Advance ACS Abstracts, October 15, 1993.